Journal of Solid State Chemistry **156,** 37–43 (2001)
doi:10.1006/jssc.2000.8955, available online at http://www.idealibrary.com on IDEAL®

Transition Metal-Substituted Lithium Pnictogenide phases. Synthesis and Crystal Structure Determinations of Novel Phases in the Li–*M*–*X* Systems (*M* = V, Nb, Ta; *X*=P, As)

Laure Monconduit,[1] Monique Tillard-Charbonnel, and Claude Belin

*Laboratoire des Agrégats Moléculaires et Matériaux Inorganiques UMR 5072, Université de Montpellier II, Sciences et Techniques du Languedoc, 2, Place E. Bataillon 34095 Montpellier Cédex 5, France

E-mail: moncondu@univ-montp2.fr, mtillard@univ-montp2.fr, cbelin@univ-montp2.fr

Received June 1, 2000; in revised form July 31, 2000; accepted September 5, 2000; published online December 21, 2000

Li–*M*–*X* systems have been investigated and crystal structures of several phases determined. Li_7NbP_4 crystallizes in the anti-fluorite-type structure (cubic, $Fm\bar{3}m$, $a = 5.996(1)$ Å, $Z = 1$, $R(F) = 3.02\%$). $LiNbAs_2$ and $Li_{4.54}V_{1.22}As_4$ display the blende-type structure, cubic $F\bar{4}3m$ space group ($LiNbAs_2$:$a = 6.309(1)$ Å, $Z = 2$, $R(F) = 2.12\%$; $Li_{4.54}V_{1.22}As_4$:$a = 6.167(1)$ Å, $Z = 1$, $R(F) = 1.49\%$). In all compounds, the transition metal statistically occupies some of the tetrahedral sites with lithium. For $Li_{4.54}V_{1.22}As_4$, one of the octahedral sites of the fcc lattice is partially filled with lithium. This feature is also observed for the homologue compounds $Li_x(Li_{3.20}Nb_{0.80})As_4$ and $Li_x(Li_{3.64}Ta_{0.36})As_4$, $0 < x \leq 4$ ($F\bar{4}3m$, $Z = 1$, $a = 6.190(3)$ and $6.184(3)$ Å, $R(F) = 1.76$ and 3.42%, respectively). © 2001 Academic Press

Key Words: **pnictogenide compounds; mixed lithium transition metal compounds; crystal structure; electronic structure.**

INTRODUCTION

Intermetallic compounds or phases containing MX_4 anions (M = transition metal, X = pnictogen atom) in association with Li cations are intermediate between ionic compounds and metallic phases and are close in properties to Zintl phases. They are expected to provide interesting electrochemical properties owing to the fluctuation of the oxidation state the transition metal may undergo when the lithium content is varied. They have recently gained particular attention as possible anode materials for rechargeable lithium batteries (1).

Most of lithium ternary pnictogenide compounds have structures that derive from the antifluorite structure type (Li_2O). Pnictogen anions X^{3-} form a face-centered cubic (fcc) lattice where the tetrahedral sites are occupied by lithium and transition metal cations, either in a disordered (C1 type, $Fm\bar{3}m$) or in an ordered (C1b type, MgAgAs (2), $F\bar{4}3m$) distribution. Formation of these networks depends on the kind of the inserted transition metal. In such cubic structures, the lithium and transition metal cations must have similar ionic radii to occupy together the tetrahedral sites. A given oxidation state for the transition metal may privilege the formation of one structural form. In LiMnAs (3) where manganese is assumed to have the $+2$ oxidation state, the tetrahedral sites are equally occupied by both cations, randomly at temperature above 500°C and even after quenching, orderly at temperatures below. The C1b ordered distribution of metal cations is very common in compounds containing late transition metals in the $+2$ oxidation state; it is the case for LiZnN, LiZnP, and LiZnAs (4, 5). A look at the arrangement of N and Zn shows a blende-like lattice (half of the tetrahedral sites occupied) in which the remaining tetrahedral sites are filled with lithium. To our knowledge, the trend for vanadium-containing ternary phases with As or P is to adopt disordered structures of type C1 (6). However, ordering of cations may occur, implying the formation of superstructures of the antifluorite type with primarily doubling of the cubic cell parameter. It is the case for compounds Li_7VN_4 (7), Li_7TaN_4 (8), and Li_7NbN_4 (9) and for several nitride phases (10).

On the other hand, many pnictogenide phases (11) may be regarded as deriving from the Li_3Bi structural type (12), which is in fact a substituted version of the NaTl structure. In Li_3Bi ($Fm\bar{3}m$), the octahedral and the tetrahedral sites of the Bi fcc lattice are filled with lithium. The same structure is found for the low-temperature Li_3Sb, while the high-temperature allotropic form is hexagonal. Curiously, only the hexagonal form is observed for Li_3As and Li_3P but we will

[1]To whom correspondence should be addressed.

0022-4596/01 $35.00

show in this work that insertion of Nb atoms in Li_3As leads to a cubic antifluorite-type ternary phase. This cubic cell results from the elongation of the c parameter of the Li_3As hexagonal cell (see below), as a lithium atom is replaced by a transition metal atom.

Vacancies in the cationic network of the cubic Li_3Bi-type ternary phases occur when, given an oxidation state greater than $+1$, the content of the transition element is varied. Stoichiometry of these phases may be denoted by the general formula $(Li_x^+ M_{(12-x)/n}^{n+} \square_{(12-x)(n-1)/n}) X_4^{3-}$ where M and X stand for transition metal and pnictogen atoms, respectively, and $\square$ for vacancies. It is likely that these deficient phases should be prone to accept additional lithium without any important structural modification (topotactic process). Either in phases deriving from the antifluorite structures where octahedral sites are left vacant or in phases deriving from the Li_3Bi frame, lithium could be inserted chemically or electrochemically as recently done for nitride phases (1). Much work is to be done relative to properties measurements (conductivity, magnetism) and electronic structure determinations in order to understand the electron transfer in these materials. The aim of this work has been, in a first stage, to prepare and characterize new ternary lithium pnictogenide phases containing transition metals of group 5 (V, Nb, Ta).

EXPERIMENTAL SECTION

Ternary phases were prepared from the elements inside niobium or tantalum tubes sealed under argon by arc welding. Except for lithium, powders of elements were used. Lithium metal (Cogema, 99.94%), niobium (Aldrich, 99.9%, 40 mesh), tantalum (Aldrich, 99.9%, 200 mesh), vanadium (Aldrich, 99.5%, 325 mesh), and red phosphorus (Merck, 98%, powder) were used without purification. Arsenic (Merck, analysis grade) was purified at 593 K under vacuum to eliminate the arsenic oxide (As_2O_3) impurities. Owing to the reactivity of pnictogens against niobium and tantalum, syntheses had to be carried out in the appropriate tubing in order to avoid formation of quaternary Nb/Ta phases. $LiNbAs_2$, Li_7NbP_4, Li_7VAs_4, Li_7NbAs_4, and Li_7TaAs_4 alloys were prepared in stoichiometric proportions by melts of lithium and pnictogens that attack the refractory metal. They were heated at 1100 K (As-containing phases) and 1000 K (P-containing phase) for 20 h and cooled quite rapidly (100°/h) to prevent the formation of relatively stable binary phases. Starting materials and products that are air and moisture sensitive were handled in an argon-filled glove box; the products appeared homogeneous. The alloys were examined under a microscope inside a dry box to select small pieces that, inserted inside Lindemann glass capillaries, were checked for singularity by X-ray diffraction techniques.

TABLE 1
Summary of Crystallographic Data for Compounds Li_7NbP_4, $LiNbAs_2$, and $Li_{4.54}V_{1.22}As_4$

Formula	Li_7NbP_4	$LiNbAs_2$	$Li_{4.54}V_{1.22}As_4$
Space group, Z	$Fm\bar{3}m$, 1	$F\bar{4}3m$, 2	$F\bar{4}3m$, 1
Molecular weight ($g.mol^{-1}$)	265.37	499.38	396.20
Lattice parameter (Å)	5.996(1)	6.309(1)	6.167(1)
Cell volume (Å^3)	215.57	251.12	234.54
Calculated density ($Mg.m^{-3}$)	2.041	3.302	2.805
Radiation λ Mo$K\alpha$ (cm^{-1})	0.71069	0.71069	0.71069
μ (mm^{-1})	2.03	15.27	15.15
Theta range (°)	5.9–34.4	5.6–27.46	5.73–34.98
Collected reflections (octant hkl)	239	143	516
Number of unique data with $I > 2\sigma(I)$	40	35	71
Equivalent reflection averaging R_{int} (%)	10.57	13.48	6.09
Number of refined parameters	4	5	7
Goodness of fit	1.25	0.95	1.18
R_1 ($I > 2\sigma(I)$) (%)	3.02	2.12	1.49
wR_2 ($I > 2\sigma(I)$) (%)	8.27	4.46	3.80
Residual electron densities	+0.62/ −0.46	+0.37/ −0.51	+0.39/ −0.27

RESULTS AND DISCUSSION

Structure Solution, Refinement, and Packing Description

For each phase, the best single crystal was mounted on an Enraf–Nonius CAD-4 automatic diffractometer, Mo$K\alpha$ radiation ($\lambda = 0.71069$ Å) for data collection. Intensities of three standard reflections were checked after every 100 reflections recorded. No significant loss was observed. Data were corrected for background, Lorentz, and polarization effects. A numerical absorption (Gaussian integration) based on indexed and measured faces was applied using the program PLATON (13) once the exact composition of the crystals were known.

For the compounds Li_7NbP_4, $LiNbAs_2$, and $Li_{4.54}V_{1.22}As_4$, crystal data are summarized in Table 1. The positional and thermal parameters are given in Table 2 and main interatomic distances in Table 3.

Li_7NbP_4. The structure of Li_7NbP_4 was solved in the centrosymmetric space group $Fm\bar{3}m$ (n°225) by the direct methods of the SHELXS 97 program (14) and refined using the program SHELXL 97 (15). This compound crystallizes in the "pure" antifluorite structure, phosphorus atoms are found at the 4a (0, 0, 0) crystallographic site with symmetry $m\bar{3}m$, and the other octahedral site 4b ($\frac{1}{2}, \frac{1}{2}, \frac{1}{2}$) is left vacant. The tetrahedral site 8c ($\frac{1}{4}, \frac{1}{4}, \frac{1}{4}$) is statistically occupied by Li and Nb in the ratio 0.86/0.14. Crystal structure is depicted in Fig. 1. Atoms Li/Nb are tetrahedrally coordinated by P atoms at 2.5963(4) Å. Furthermore, they are surrounded by a Li/Nb octahedron at 2.9980(5) Å and by a Li/Nb

TABLE 2
Positional and thermal parameters for atoms in Li_7NbP_4, $LiNbAs_2$ and $Li_{4.54}V_{1.22}As_4$

Atom	Position	x	y	z	U_{eq}	sof
Li_7NbP_4 ($Fm\bar{3}m$)						
P	4(a)	0	0	0	0.0201(6)	1.0
Li	8(c)	$\frac{1}{4}$	$\frac{1}{4}$	$\frac{1}{4}$	0.0094(6)	0.863(3)
Nb	8(c)	$\frac{1}{4}$	$\frac{1}{4}$	$\frac{1}{4}$	0.0094(6)	0.137(3)
$LiNbAs_2$ ($F\bar{4}3m$)						
As	4(a)	0	0	0	0.011(1)	1.0
Li	4(c)	$\frac{3}{4}$	$\frac{3}{4}$	$\frac{3}{4}$	0.008(2)	0.49(1)
Nb	4(c)	$\frac{3}{4}$	$\frac{3}{4}$	$\frac{3}{4}$	0.008(2)	0.51(1)
$Li_{4.54}V_{1.22}As_4$ ($F\bar{4}3m$)						
As	4(a)	0	0	0	0.0187(3)	1.0
Li1	4(c)	$\frac{1}{4}$	$\frac{1}{4}$	$\frac{1}{4}$	0.017(1)	0.69(1)
V	4(c)	$\frac{1}{4}$	$\frac{1}{4}$	$\frac{1}{4}$	0.017(1)	0.31(1)
Li2	4(b)	$\frac{1}{2}$	$\frac{1}{2}$	$\frac{1}{2}$	0.03(1)	0.44(1)

Note. General expression of the thermal parameter is $\exp[-2\pi^2(U_{11}h^2a^{*2} + U_{22}k^2b^{*2} + U_{33}l^2c^{*2} + 2U_{12}hka^*b^* + 2U_{13}hla^*c^* + 2U_{23}klb^*c^*]$. $U_{eq} = [\sum_i \sum_j U_{ij}a_i^*a_j^*\bar{a}_i.\bar{a}_j]/3$.

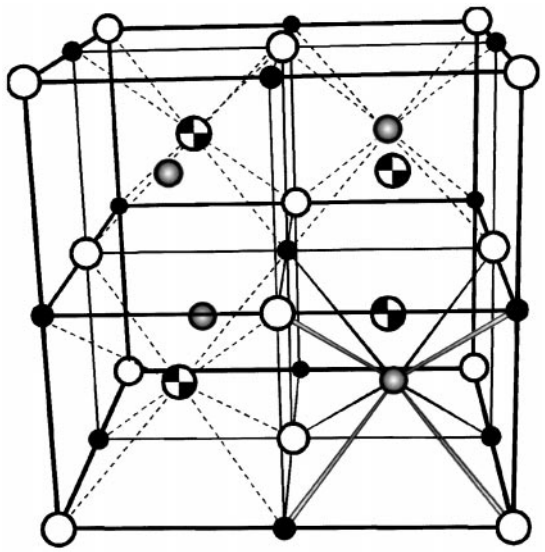

FIG. 1. Representation of a fcc unit cell. The fcc lattice is represented by the positions ◯, the octahedral sites by ●, and the tetrahedral sites by ◔ and ◍. In the ZnS blende structure type, only the (0, 0, 0) and $(\frac{1}{4}, \frac{1}{4}, \frac{1}{4})$ positions are occupied by S and Zn atoms, respectively. In the Li_2O antifluorite structure type, the oxygen atom forms the fcc lattice, and the Li atoms occupy the $(\frac{1}{4}, \frac{1}{4}, \frac{1}{4})$ and $(\frac{3}{4}, \frac{3}{4}, \frac{3}{4})$ tetrahedral sites. Li_7NbP_4, ◯ = P, ◔, ◍ = Li/Nb; $LiNbAs_2$, ◯ = As, ◔ = Li/Nb; $Li_{4.54}V_{1.22}As_4$, ◍ = P, ◯ = Li/Nb; ● = Li (idem for $Li_x(Li_{3.20}Nb_{0.80})As_4$ and $Li_x(Li_{3.64}Ta_{0.36})As_4$).

cuboctahedron at 4.2398(7) Å (Fig. 2). Around the phosphorus atom, consecutive shells are a Li/Nb cube at 2.5963(4) Å and a P cuboctahedron at 4.2398(7) Å (Fig. 2).

$LiNbAs_2$. The compound $LiNbAs_2$ crystallizes in the blende structure type (noncentrosymmetric $F\bar{4}3m$ space group, n°216). In Fig. 3 the consecutive coordination shells around the different atoms are represented. The As atom lies at 4a (0, 0, 0) position, and Nb and Li statistically occupy ($\approx$ 50/50) the 4d $(\frac{3}{4}, \frac{3}{4}, \frac{3}{4})$ site. Refinement of these positions (assumed to be the true absolute configuration) gave a $R(F)$ reliability factor of 2.12% and a flack parameter of 0.20(6). Refinement of the inverse configuration only gave a $R(F)$ factor of 4.36% and a flack parameter of 0.65(13). Each arsenic atom ($\bar{4}3m$ site) is tetrahedrally surrounded by four Li/Nb at 2.7319(4) Å and furthermore, by 12 arsenic atoms at 4.4611(7) Å that form a cuboctahedron. The 4c site also has the $\bar{4}3m$ symmetry, implying for Li/Nb atoms a similar environment, i.e., 4 As at 2.7319(4) Å and 12 Li/Nb at 4.4611(7) Å.

$Li_{4.54}V_{1.22}As_4$. According to extinction conditions, the only possible space groups were noncentrosymmetric $F23$, $F432$, and $F\bar{4}3m$ and centrosymmetric $Fm\bar{3}$ and $Fm\bar{3}m$. The centrosymmetric groups would afford more disordered distributions of atoms and vacancies. Although the statistical tests for centrosymmetry provided by SHELXS 97 and based on the mean $|E^*E - 1|$ clearly indicated the structure to be noncentrosymmetric, the centrosymmetric space groups were yet checked for refinements and proved inappropriate. Intensity data averaged well for the $m\bar{3}m$ ($R_{int} = 0.061$) as well as for the lower Laue symmetry $m\bar{3}$ ($R_{int} = 0.059$). The structure refined equally in the $F23$ and $F\bar{4}3m$ space groups with respectively $R(F)$ of 0.0165 for 90 independent reflections and 0.0149 for 71 independent reflections. Hence, the noncentrosymmetric $F\bar{4}3m$ space group has been retained to describe the structure of $Li_{4.54}V_{1.22}As_4$ ($Li_{1.76}(Li_{2.78}V_{1.22})As_4$). The absolute configuration of this compound could not be determined.

TABLE 3
Main Distances (Å) Less than 5 Å in Li_7NbP_4, $LiNbAs_2$, and $Li_{4.54}V_{1.22}As_4$ Compounds

	X–X	M–X	Li_1–X	Li_1–Li_1	Li_1–Li_2	M–Li_2	Li_2–X	Li_1–M
Li_7NbP_4	4.2398(7)	2.5963(4)	2.5963(4)	2.9980(5)				2.9980(5)
$LiNbAs_2$	4.4611(7)	2.7319(4)	2.7319(4)	4.4611(7)				4.4611(7)
$Li_{4.54}V_{1.22}As_4$	4.3607(7)	2.6704(4)	2.6704(4)	4.3607(7)	2.6704(4)	2.6704(4)	3.0835(5)	4.3607(7)

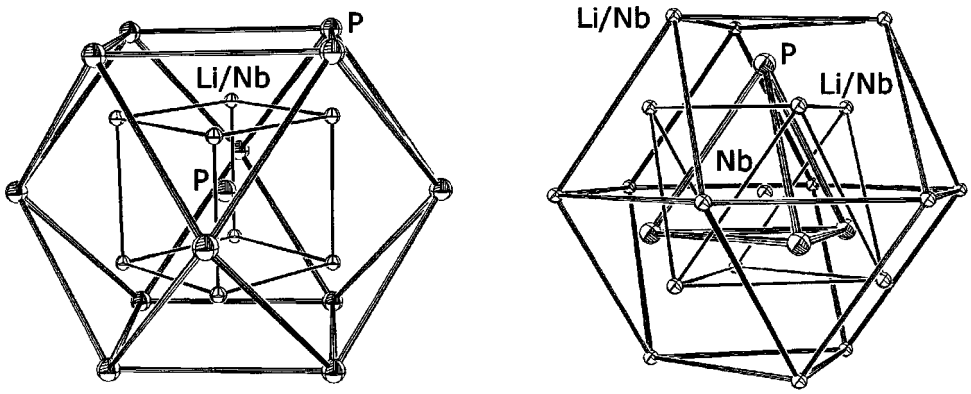

FIG. 2. Representation of the atomic environments in Li_7NbP_4. (Left) The Li/Nb cube and P cuboctahedron around P atom. (Right) The P tetrahedron, Li/Nb octahedron, and Li/Nb cuboctahedron around Li/Nb position.

Both metals, Li1 and V, randomly occupy the 4c site $(\frac{1}{4}, \frac{1}{4}, \frac{1}{4})$ in the ratio $\frac{70}{30}$ and the arsenic atom lies at the 4a position (0, 0, 0). As is the case in blende structure, the 4d site is left vacant. However, site 4b $(\frac{1}{2}, \frac{1}{2}, \frac{1}{2})$ is found to be partially filled by supplementary lithium (1.8 atoms per unit cell). The corresponding atom Li2 lies at the center of concentric shells: a Li1/V tetrahedron at 2.6704(4) Å, an As octahedron at 3.0835(5) Å, and a Li2 cuboctahedron at 4.3607(5) Å (Fig. 4). Each As atom is concentrically surrounded by four Li1/V on a tetrahedron at $(a\sqrt{3})/4$ (2.6704(4) Å), six Li2 on an octahedron at $a\sqrt{2}$ (3.0835(5) Å) and 12 As on a cuboctahedron at $(a\sqrt{2})/2$ (4.3607(7) Å). The coordination shells around the Li1/V atom are somewhat different (to be compared with the phosphorus environment in the centrosymmetric $Fm\bar{3}m$ structure). Each Li1/V atom is surrounded at 2.6704(4) Å by an As tetrahedron and a Li2 tetrahedron (that form a cube), and further at 4.3607(7) Å by a Li1/V cuboctahedron.

$Li_x(Li_{3.20}Nb_{0.80})As_4$ and $Li_x(Li_{3.64}Ta_{0.36})As_4$, $0 < x \leq 4$. For these two compounds, single crystals have been found to display the cubic symmetry, $F\bar{4}3m$ space group. The cell dimensions, 6.190(3) and 6.184(3) Å, respectively, are slightly larger than that of the vanadium compound $Li_{4.54}V_{1.22}As_4$ (6.167(1) Å). As expected, the unit cell parameter increases with the transition metal cation size; ionic radii of V^{5+}, Nb^{5+}, and Ta^{5+} are respectively 0.495, 0.620, and 0.620 Å, which implies the As fcc framework to be a little more compact in the vanadium compound than in the niobium and tantalum homologues.

The two compounds were assumed to have structures close to that of the vanadium compound; both metals, namely Li and Nb (or Ta), randomly occupy the 4c site $(\frac{1}{4}, \frac{1}{4}, \frac{1}{4})$ in the ratio $\frac{80}{20}$ (niobium compound) and $\frac{91}{9}$ (tantalum compound) while the arsenic atom lies at the 4a position (0, 0, 0). The last Fourier difference displayed, for both compounds, a small residual at $(\frac{1}{2}, \frac{1}{2}, \frac{1}{2})$ that might be assigned to

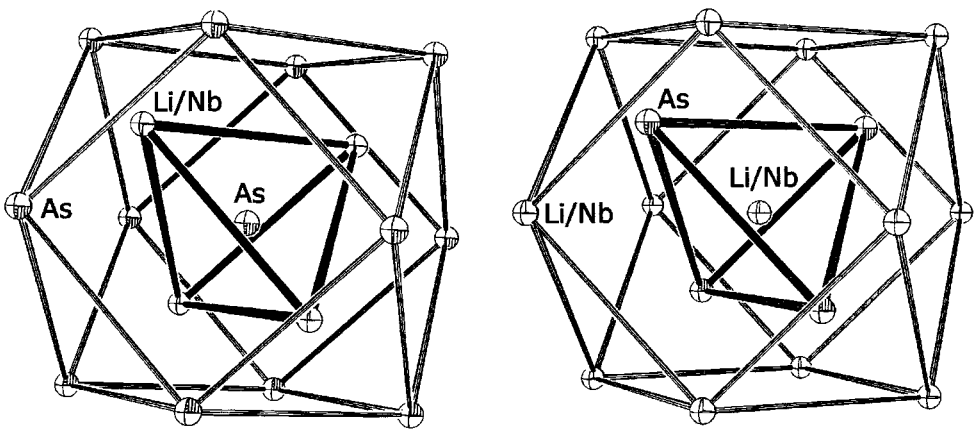

FIG. 3. Representation of the atomic environments in $LiNbAs_2$. (Left) The Li/Nb tetrahedron and As cuboctahedron around As atom. (Right) The As tetrahedron and Li/Nb cuboctahedron around Li/Nb position.

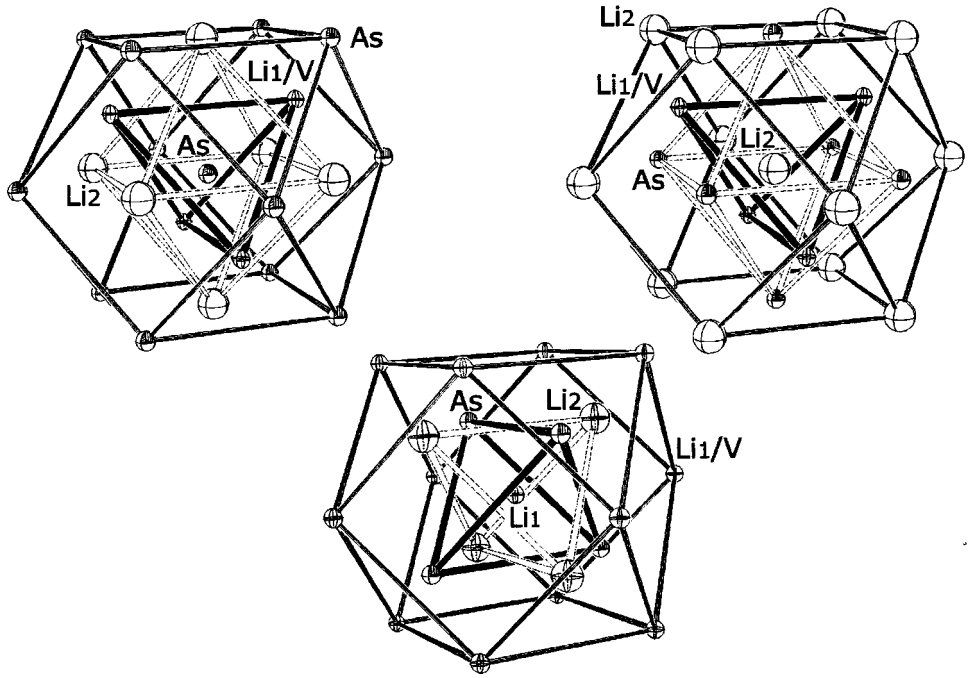

FIG. 4. Representation of the atomic environments in $Li_{4.54}V_{1.22}As_4$. (Top left) The Li1/V tetrahedron, Li2 octahedron, and As cuboctahedron around As atom. (Top right) The Li1/V tetrahedron, As octahedron, and Li2 cuboctahedron around Li2 atom. (Bottom) The As and Li tetrahedra and Li1/V cuboctahedron around Li1/V position.

some extra lithium. The 4d site remains vacant as indicated by the absence of residual electron density at $(\frac{3}{4}, \frac{3}{4}, \frac{3}{4})$. Although the least-squares refinements have been carried out to $R_1 = 1.76$ and 3.42% for the niobium and tantalum compounds, respectively, it was not possible to determine the lithium content on the 4b site and to give the accurate crystallographic formula.

Relation between the Li_7MAs_4, and Li_3As Structures

Starting from Li_3As (16), the replacement of some lithium by a heavy metal atom M ($Li_{12}As_4 \rightarrow Li_7M^{V}As_4$) induces a transformation of the hexagonal cell into a fcc cell, the matrix is

$$\begin{bmatrix} \frac{4}{3} & \frac{2}{3} & \frac{1}{3} \\ -\frac{2}{3} & \frac{2}{3} & \frac{1}{3} \\ -\frac{2}{3} & -\frac{4}{3} & \frac{1}{3} \end{bmatrix}.$$

This proceeds by a consequent lengthening of the hexagonal c parameter, 7.81 to 10.73 Å, for the body diagonal of the cube.

Strikingly, among the five phases reported in this work, Li_7NbP_4 is the only one that adopts the pure antifluorine structure ($Fm\bar{3}m$) as do lots of compounds reported by Juza *et al.* (10). Actually, Li_7VAs_4 and LiZnAs arsenides were claimed to display the $Fm\bar{3}m$ symmetry, but their structures were poorly determined on the basis of X-ray powder data (4, 6). From single-crystal data (5), it was recently shown that LiZnAs has a filled-up blende structure type ($F\bar{4}3m$) in which Li and Zn occupy the 4c and 4d sites, respectively.

For the $F\bar{4}3m$ arsenide phases described in this work, only one of the 4c $(\frac{1}{4}, \frac{1}{4}, \frac{1}{4})$ or 4d $(\frac{3}{4}, \frac{3}{4}, \frac{3}{4})$ sites is always found empty while the other is statistically occupied by lithium and the transition metal. The site 4b $(\frac{1}{2}, \frac{1}{2}, \frac{1}{2})$, which has the same symmetry ($\bar{4}3m$) as 4c and 4d, is empty (in $LiNbAs_2$) or partially filled (in $Li_{4.54}V_{1.22}As_4$ and in Nb and Ta homologues).

Pauling's electronegativities for metals and Li (M), V, Nb, Ta are 1.0, 1.6, 1.6, 1.5, respectively; they are 3.0, 2.1, and 2.0 for pnictogens (X) N, P, and As. According to the differences in electronegativity, a more covalent bonding is expected between M and X than between Li and X. In the nitride compounds Li_7TaN_4 (8) and Li_7NbN_4 (9) bonding is assumed to be ionic and, despite the smaller radius of nitrogen, packing is less compact. In all these structures, the transition metal atoms M are bonded to four pnictogens, forming tetrahedral MX_4 anions. Usually, such discrete anions are described with 32 valence electrons that gives a formal anionic charge -7 for VX_4, NbX_4, and TaX_4 anions. This is verified for Li_7NbP_4 but not for $Li_{4.54}V_{1.22}As_4$. In the case of $LiNbAs_2$, formally described as $2Li^+$, $[Nb_2As_4]^{2-}$, the unit cell contains two Nb atoms and the NbX_4 tetrahedra are no longer discrete but fused by

edge-sharing. So far, owing to these various stoichiometry situations and also to the nature of the cationic species, description of these phases either as ionic (discrete Li^+, M^{5+}, and X^{3-} ions) or as partially covalent (molecular MX_4 or M_2X_6 anions) structures is not achieved. Theoretical calculations are in progress to interpret the cationic deficiency in $Li_{4.54}V_{1.22}As_4$ and in some related compounds (17).

Electronic Band Calculations

In order to have a better understanding of what would occur in these structures during a lithiation process, we have performed a preliminary tight-binding band structure analysis. Calculations have been carried out for the compound $LiNbAs_2$ because it has a large number of available sites to host lithium atoms. Our calculations used an effective Hamiltonian of the extended Hückel type (18) with the following parameters H_{ii}(eV) and exponents ζ:As 4*s* −16.219, 2.23; As 4*p* −12.16, 1.89; Nb 5*s* −10.1, 1.89; Nb 5*p* −6.86, 1.85; Nb 4*d* −12.10, 4.08 (0.6401), 1.64 (0.5516). The nondiagonal H_{ij} matrix elements were calculated by means of the modified Wolfsberg–Helmholz formula (19). The most electropositive atoms (lithium) were considered as one-electron donors and then not included in calculations.

First, we have built periodic models that take into account the $\frac{50}{50}$ disorder of Nb and Li at position $(\frac{3}{4}, \frac{3}{4}, \frac{3}{4})$. There are two lithium and two niobium atoms distributed at the apices of a tetrahedron around the $(\frac{1}{2}, \frac{1}{2}, \frac{1}{2})$ center of the unit cell. Whatever is the arrangement of these atoms, one over the six tetrahedron edges always contains two Nb atoms. Each of these Nb–Nb edges occurs once in the chosen periodic model built on a repeat unit of $3 \times 2 \times 1$ cubic cells. Although it may appear somewhat artificial, this model containing 24 As and 12 Nb atoms provides a relatively good description of the occupational disorder. Nb atoms are always tetrahedrally coordinated by As atoms at 2.732 Å, while various coordinations are found for As atoms. There are 1 noncoordinated, 4 one-coordinated, 14 two-coordinated, 4 three-coordinated, and 1 four-coordinated As atoms. Note that the choice of any other large cell model would not significantly modify the overall coordination.

The densities of states (20) have been calculated with a set of 216 *k* points taken in the irreducible part of the Brillouin zone (k_x, k_y, k_z varying from 0 to 0.5). Figure 5 represents the total and projected densities of states (DOS). It displays two groups of bands separated by nearly 1 eV. The considered model contains 12 $LiNbAs_2$ units, then 192 valence electrons are available for stabilization of the $NbAs_2$ framework. The corresponding Fermi level lies on a sharp band staying at an energy close to the As 4*p* ionization potential. This band corresponds to lone pairs at the noncoordinated

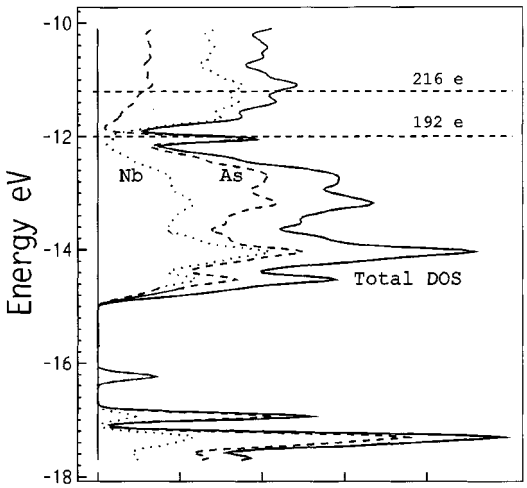

FIG. 5. Total densities of states (DOS) calculated for a large ordered model of $LiNbAs_2$ and projected DOS for Nb and As atoms. The Fermi level is indicated for 192 valence electrons $(LiNbAs_2) \times 12$ and for a hypothetical 216 electron filling $(Li_3NbAs_2) \times 12$.

As atom (As^{3-}); complementarily, the As 4*s* atomic orbital is observed as a sharp band at −16.2 eV. The comparison of the DOS shapes is interesting, the good match of the partial DOS of Nb with that of As (excluded are the two sharp bands at −12 and −16.2 eV assigned to the As nonbonding pairs) points out the covalent nature of the Nb–As interactions.

A complementary and more informative analysis of the electronic structure is provided by the crystal orbital overlap populations (COOP) (21) calculated for different types of interactions. They tell us about the bonding, nonbonding, or antibonding nature of the interactions. Figure 6 clearly indicates the bonding character of the Nb–As interactions up to the Fermi level (192 e); it also shows that there is no significant Nb–Nb nor As–As overlapping. Insertion of supplementary lithium in the $LiNbAs_2$ compound would process by the reduction of the host lattice $[NbAs_2]$, raising the question of the location of additional charges. Since there is room at 4b $(\frac{1}{2}, \frac{1}{2}, \frac{1}{2})$ or at 4c $(\frac{1}{4}, \frac{1}{4}, \frac{1}{4})$, let us imagine that we could insert at least four additional lithium atoms per unit cell; it would fill our repeat unit ($3 \times 2 \times 1$ model) with 24 Li atoms, increasing the overall valence electron number from 192 to 216. The Fermi level for 216 electrons (Fig. 6) lies in the antibonding (mainly Nb–As) domain. Nevertheless the difference in the overlap population calculated for Nb–As bonds, 0.785 for 192 electrons and 0.774 for 216 electrons, is not very important, indicating that the insertion of extra lithium would not consistently destabilize the host matrix.

On the other hand, analysis of DOS projections for arsenic having different coordination modes and niobium atoms shows that electron transfer mainly affects the transition metal (gain of 1.64 electron per Nb). Arsenic

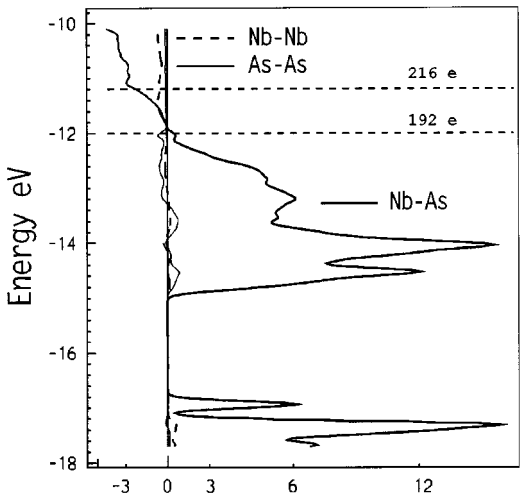

FIG. 6. Crystal orbital overlap populations (COOP) for bonds Nb–As (bold line), As–As (thin line), and Nb–Nb (dotted line) in $LiNbAs_2$. The Fermi level is indicated for 192 valence electrons $(LiNbAs_2) \times 12$ and for a hypothetical 216 electron filling $(Li_3NbAs_2) \times 12$.

atoms that have lowest coordination numbers are slightly reduced (gain of 0.26 e for one-coordinated As and 0.18 for two-coordinated As atoms).

CONCLUDING REMARKS

Our structural analyses show how filling of the various $\bar{4}3m$ sites is versatile in the sense that the mixed ternary Li/*M* pnictogenides are close to being solid solutions. In these phases, lithium may occupy any $\bar{4}3m$ site without structural modification, which would be favorable to a topotactic insertion/desinsertion of supplementary lithium in the unit cell. These compounds are interesting as potential negative electrodes in lithium rechargeable batteries. It is well known that the cycling performances of an anodic material is significantly improved when using ternary intermetallic compounds or composite host materials. This avoids the problems associated with the volume expansion/contraction on cycling of the Li_xM alloy or graphite-based electrodes. First attempts to insert supplementary Li showed that $Li_{4.54}V_{1.22}As_4$ can accept up to four Li atoms per formula without any structural modification of the host lattice (the X-ray diffraction pattern is not affected by the inserted atoms). Electrochemical studies of these compounds are in progress in order to determine their performances as anodes and their behaviour on lithium insertion/desinsertion processes. Because they contain elements that are toxic in nature, these materials will be studied only as experimental and model electrodes.

REFERENCES

1. M. Nishijima, T. Tagohashi, Y. Takeda, M. Imanishi, and O. Yamamoto, *J. Power Sources* **68,** 510 (1997).
2. H. Nowotny and W. Sibert, *Z. Metallk.* **33,** 391 (1941).
3. R. Juza, W. Dethlefsen, H. Seidel, and K. von Benda, *Z. Anorg. Allg. Chem.* **356,** 253 (1968).
4. H. Nowotny and K. Bachmeyer, *Monatsh. Chem.* **81,** 488 (1950).
5. W. Hönle, *Z. Naturforsch. B* **48,** 683 (1993).
6. R. Juza and W. Uphoff, *Z. Anorg. Chem.* **292,** 65 (1957).
7. R. Juza, W. Gieren, and J. Haug, *Z. Anorg. Chem.* **300,** 61 (1959).
8. C. Wachsmann, H. Jacobs, *J. Alloys Compds.* **190,** 113 (1992).
9. D. A. Vennos and F. J. DiSalvo, *Acta Crystallogr. Sect. C* **48,** 610 (1992).
10. R. Juza, K. Langer, and K. von Benda, *Angew. Chem. Int. Ed.* **7,** 5 (1968).
11. R. Juza and K. Langer, *Z. Anorg. Allg. Chem.* **361,** 74 (1968).
12. E. Zintl and G. Brauer, *Z. Phys. Chem. B* **37,** 323 (1937).
13. A. L. Spek, *Acta Crystallogr. Sect. A* **46,** C-34 (1990).
14. G. M. Sheldrick, "SHELXS-97, Program for Crystal Structure Determination." Göttingen, Germany, 1997.
15. G. M. Sheldrick, "SHELXL-97, Program for Crystal Structure Refinement." Göttingen, Germany, 1997.
16. G. Brauer and E. Zintl, *Z. Phys. Chem. B* **37,** 323, (1937).
17. M. L. Doublet, S. Rémy, and L. Monconduit, to be published.
18. R. Hoffmann, *J. Chem. Phys.* **39,** 1397 (1963).
19. J. H. Ammeter, H.-B. Bürgi, J. C. Thiebeault, and R. Hoffmann, *J. Am. Chem. Soc.* **100,** 3686 (1978).
20. R. Hoffmann, *Angew. Chem. Int. Ed.* **26,** 846 (1987).
21. T. Hughbanks and R. Hoffmann, *J. Am. Chem. Soc.* **105,** 1150 (1983).